

# Secular theory of the orbital evolution of the young stellar disc in the Galactic Centre

J. Haas<sup>1\*</sup>, L. Šubr<sup>1,2</sup> and D. Vokrouhlický<sup>1</sup>

<sup>1</sup>*Astronomical Institute, Faculty of Mathematics and Physics, Charles University, V Holešovičkách 2, 18000 Praha, Czech Republic*

<sup>2</sup>*Astronomical Institute, Academy of Sciences, Boční II, 14131 Praha, Czech Republic*

Accepted —. Received —; in original form —

## ABSTRACT

We investigate the orbital evolution of a system of  $N$  mutually interacting stars on initially circular orbits around the dominating central mass. We include perturbative influence of a distant axisymmetric source and an extended spherical potential. In particular, we focus on the case when the secular evolution of orbital eccentricities is suppressed by the spherical perturbation. By means of standard perturbation methods, we derive semi-analytic formulae for the evolution of normal vectors of the individual orbits. We find its two qualitatively different modes. Either the orbits interact strongly and, under such circumstances, they become dynamically coupled, precessing synchronously in the potential of the axisymmetric perturbation. Or, if their mutual interaction is weaker, the orbits precess independently, interchanging periodically their angular momentum, which leads to oscillations of inclinations. We argue that these processes may have been fundamental for the evolution of the disc of young stars orbiting the supermassive black hole in the centre of the Milky Way.

**Key words:** methods: analytical – celestial mechanics – stars: kinematics and dynamics – Galaxy: nucleus.

## 1 INTRODUCTION

Problem of dynamics in the perturbed Keplerian potential has been studied extensively throughout the history of celestial mechanics. Due to high attainable accuracy of observational data, its primary field of application has always been the Solar System, which naturally influenced the selection of included perturbations. Ones of those widely considered are, due to their resemblance with the averaged motion of planets, axisymmetric gravitational potentials.

The above problem has, however, also been investigated for systems with larger length scales, such as dense star clusters. In that case, the source of the Keplerian potential is often represented by a supermassive black hole (SMBH) which is widely assumed to reside in the centres of such clusters. Axisymmetric perturbation is then either due to a secondary massive black hole (e.g. Ivanov, Polnarev & Saha 2005) or a gaseous disc or torus (e.g. Karas & Šubr 2007). It turns out that in these systems, the secular evolution of individual stellar orbits is, beside the axisymmetric perturbation, also affected by a possible additional spherical potential. Such a potential may be generated by a stellar cusp or it can represent a post-Newtonian correction to the gravity of the central black hole.

In this paper, we extend the analyses of previous authors by means of standard tools of celestial mechanics. Our main aim is to incorporate mutual interaction of stars on nearly-circular orbits around the dominating central mass whose potential is perturbed by a distant axisymmetric source and an extended spherical potential. We apply our results to the observed system of young stars (Genzel et al. 2003; Ghez et al. 2005; Paumard et al. 2006; Bartko et al. 2009, 2010) orbiting the SMBH of mass  $M_{\bullet} \approx 4 \times 10^6 M_{\odot}$  (Ghez et al. 2003; Eisenhauer et al. 2005; Gillessen et al. 2009a,b; Yelda et al. 2010) in the centre of the Milky Way. As an axisymmetric perturbation to its gravity we consider a massive molecular torus (the so-called circumnuclear disc; CND) which is located at radius  $R_{\text{CND}} \approx 1.8$  pc from the centre (Christopher et al. 2005). Finally, we consider gravity of a roughly spherical cusp of late-type stars (Genzel et al. 2003; Schödel et al. 2007; Do et al. 2009) which is believed to be present in this region, as well. Within this context, we broaden the analysis of our previous paper (Haas, Šubr & Kroupa 2011) where we have studied the dynamical evolution of this kind of system purely by means of numerical  $N$ -body calculations. In particular, we now develop a simple semi-analytic model which naturally explains key features of our prior results.

The paper is organized as follows. In the theoretical Section 2, we first discuss the influence of the spherical per-

\* E-mail: haas@sirrah.troja.mff.cuni.cz

turbative potential upon the stellar orbits (Section 2.1). This allows us to separate the evolution of eccentricity from the rest of the problem and, subsequently, to formulate equations for the evolution of inclinations and nodal longitudes (Section 2.2). In Section 3, we present an example of the orbital evolution of a stellar disc motivated by the configuration that is observed in the Galactic Centre. We conclude our results in Section 4.

## 2 THEORY

To set the stage, we first develop a secular theory of orbital evolution for two (later in the section generalized to multiple) stars orbiting a massive centre, the SMBH, taking into account their mutual gravitational interaction and perturbations from the spherical stellar cusp and the axisymmetric CND. The CND is considered stationary and its model is further simplified and taken equivalent to a ring at a certain distance from the centre. It should be, however, pointed out that generalization to a more realistic structure, such as thin or thick disc, is straightforward in our setting but we believe at this stage it would just involve algebraic complexity without bringing any new quality to the model. In the same way, the stellar cusp is reduced to an equilibrium spherical model without involving generalizations beyond that level. For instance, an axisymmetric component of the stellar cusp may be effectively accounted for by the CND effects in the first approximation.

We are going to use standard tools of classical celestial mechanics, based on the first-order secular solution using the perturbation methods (see, e.g., Morbidelli 2002 or Bertotti, Farinella & Vokrouhlický 2003 for general discussion). In particular, the stellar orbits are described using a conventional set of Kepler's elements which are assumed to change according to Lagrange equations. Since we are interested in a long-term dynamical evolution of the stellar orbits we replace the perturbing potential (or potential energy) with its average value over one revolution of the stars about the centre, which is the proper sense of addressing our approach as secular. In doing so, we assume there is no orbital mean motion resonance between the two (or multiple) stars. As an implication of our approach, the orbital semi-major axes of the stellar orbits are constant and information about the position of the stars in orbit is irrelevant. The secular system thus consists of description how the remaining four orbital elements, eccentricity, inclination, longitude of node and argument of pericentre, evolve in time. This is still a very complicated problem in principle, and we shall adopt simplifying assumption that will allow us to treat the eccentricities and pericentres separately (Section 2.1) and leave us finally with the problem of dynamical evolution of inclinations and nodes (Section 2.2). Note this is where our approach diverges from typical applications in planetary systems, in which this separation is often impossible.

### 2.1 Confinement of eccentricity

In this section we discuss our assumptions about eccentricity and pericentre evolution. For this moment, we drop the mutual interaction of stars from our consideration. We assume that the initial stellar orbits have small eccentricity and we

describe under which conditions we may assume they stay small to the point we could neglect them. Note this is not an obvious conclusion because axially symmetric systems (such as a perturbing massive ring) have been extensively studied in planetary applications and it has been shown that non-conservation of the total orbital angular momentum may lead to a large, correlated variations of eccentricity and inclination even if the initial eccentricity is arbitrarily small. This is often called Kozai secular resonance as a tribute to a pioneering work of Kozai (1962) (see also Lidov 1962). In what follows we describe conditions under which this process is inhibited in our model.

#### 2.1.1 Stellar cusp potential

We start with our assumption about the potential energy of a star of mass  $m$  in the spherical cusp of the late-type stars surrounding the centre. Considering a general power-law radial density profile of the cusp,  $\rho(r) \propto r^{-\alpha}$ , we have the potential energy

$$\mathcal{R}_c = -\frac{GmM_c}{\beta R_{\text{CND}}} \left( \frac{r}{R_{\text{CND}}} \right)^\beta, \quad (1)$$

where  $\beta = 2 - \alpha$ , the cusp mass within a scale distance  $R_{\text{CND}}$  is denoted  $M_c$  and  $G$  stands for the gravitational constant. According to the averaging technique, we shall integrate the potential energy (1) over one revolution about the centre with respect to the mean anomaly  $l$ ,

$$\overline{\mathcal{R}}_c \equiv \frac{1}{2\pi} \int_{-\pi}^{\pi} dl \mathcal{R}_c, \quad (2)$$

which yields

$$\overline{\mathcal{R}}_c = -\frac{1}{2\pi} \frac{GmM_c}{\beta R_{\text{CND}}} \left( \frac{a}{R_{\text{CND}}} \right)^\beta \int_{-\pi}^{\pi} dl \left( \frac{r}{a} \right)^\beta, \quad (3)$$

where  $a$  and  $e$  are semi-major axis and eccentricity of the stellar orbit,  $r = a(1 - e \cos u)$  and  $u - e \sin u = l$ . After an easy algebra, we obtain

$$\overline{\mathcal{R}}_c = -\frac{GmM_c}{\beta R_{\text{CND}}} \left( \frac{a}{R_{\text{CND}}} \right)^\beta \mathcal{J}(e, \beta), \quad (4)$$

where

$$\mathcal{J}(e, \beta) \equiv \frac{1}{\pi} \int_0^\pi du (1 - e \cos u)^{1+\beta} = 1 + \sum_{n \geq 1} a_n e^{2n}, \quad (5)$$

with the coefficients obtained by recurrence

$$\frac{a_{n+1}}{a_n} = \left[ 1 - \frac{3 + \beta}{2(n+1)} \right] \left[ 1 - \frac{2 + \beta}{2(n+1)} \right] \quad (6)$$

and an initial value  $a_1 = \beta(1 + \beta)/4$ . For the purpose of our study, we further set  $\beta = 1/4$  which corresponds to the equilibrium model worked out by Bahcall & Wolf (1976).

#### 2.1.2 Circumnuclear disc/ring potential

In the case of perturbation of orbits well below the radius of the CND, we limit ourselves to account for the quadrupole-tide formulation (e.g. Kozai 1962; Morbidelli 2002). Octupole or higher-multipole corrections are possible (e.g. in

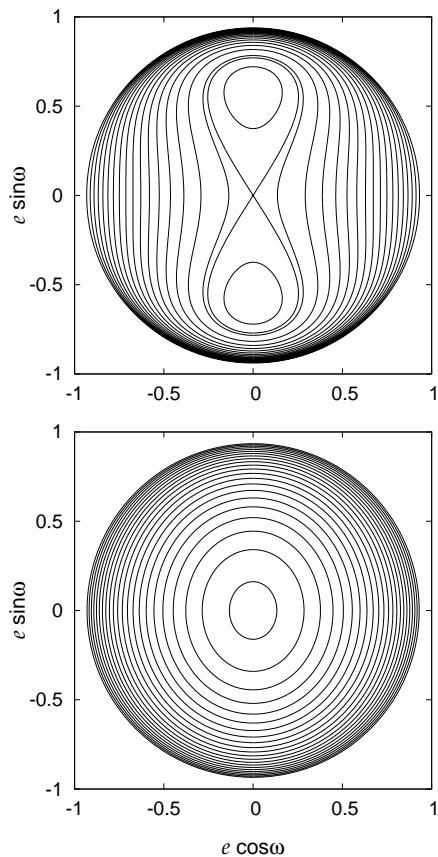


**Figure 1.** Isolines of the conserved potential function  $\overline{\mathcal{R}} = C$  from equation (9) for two different values of the mass ratio  $\mu = M_c/M_{\text{CND}}$ : 0.01 at the top panel, 0.1 at the bottom panel. The Kozai integral value is  $c = \cos(70^\circ)$ , corresponding to  $70^\circ$  inclination circular orbit. The orbit has been given semi-major axis  $a = 0.06 R_{\text{CND}}$  for sake of definiteness. The origin  $e = 0$  is a stationary point of the problem but in the first case it is unstable, while in the second case it becomes stable. The thick isoline in the top panel is a separatrix between two different regimes of eccentricity and pericentre evolution.

fact Kozai himself gives explicit terms up to degree 4; see also Yokoyama et al. 2003) but they do not change the conclusions as long as the parameter  $a/R_{\text{CND}}$  is small enough. This is the regime that interests us most.

Given the axial symmetry of the mass distribution of the perturbing ring, the resulting averaged interaction potential energy of a particle in the tidal field of the CND (see Kozai 1962)

$$\overline{\mathcal{R}}_{\text{CND}} = -\frac{GmM_{\text{CND}}}{16R_{\text{CND}}} \left(\frac{a}{R_{\text{CND}}}\right)^2 \left[ (2 + 3e^2)(3\cos^2 I - 1) + 15e^2 \sin^2 I \cos 2\omega \right] \quad (7)$$

does not depend on longitude of node  $\Omega$  but depends on other orbital elements of the stellar orbit – eccentricity  $e$ , inclination  $I$  and argument of pericentre  $\omega$ .

As a direct consequence,  $c \equiv \sqrt{1 - e^2} \cos I$  is the first (‘Kozai’) integral of motion, which conveniently allows to eliminate inclination dependence in  $\overline{\mathcal{R}}_{\text{CND}}$ , depending then on the eccentricity and argument of pericentre only. Since  $\overline{\mathcal{R}}_{\text{CND}}$  is a conserved quantity in the secular (orbit-averaged)

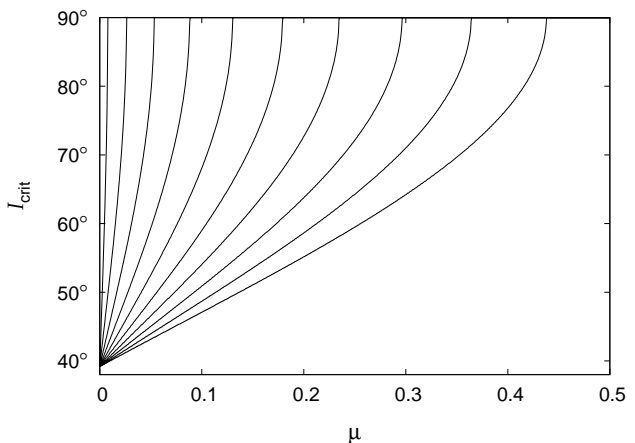


**Figure 2.** Individual lines show a critical inclination (ordinate) at which Kozai resonance onsets for a given value of mass ratio  $\mu = M_c/M_{\text{CND}}$  (abscissa) for different values of orbital semi-major axis  $a$  ranging from  $0.03 R_{\text{CND}}$  (left) to  $0.3 R_{\text{CND}}$  (right) with the step of  $0.03 R_{\text{CND}}$ . When  $\mu = 0$ , the critical angle is  $\approx 39.2^\circ$  (‘the Kozai limit’) independently from  $a$ .

problem, the isolines  $\overline{\mathcal{R}}_{\text{CND}} = C$  provide insights in the fundamental features of the dynamical evolution of both  $e$  and  $\omega$ . This approach has been used by Kozai to discover two modes of topology of these isolines: (i) when  $c > \sqrt{3/5}$  the  $\overline{\mathcal{R}}_{\text{CND}} = C$  isolines are simple ovals about origin which is the only fixed point of the problem but (ii) for  $c \leq \sqrt{3/5}$  they become more complicated with a separatrix curve emerging from the origin and two new fixed points exist at nonzero eccentricity and pericentre argument values  $90^\circ$  and  $270^\circ$ . The latter case occurs whenever the initial inclination is larger than  $\approx 39.2^\circ$ , sometimes called the Kozai limit. The important take-away message is that the circular orbit is no more a stable solution for high-inclination orbits in the model of exterior ring/disc perturbation. Initially circular orbits would be driven over a Kozai timescale

$$T_{\text{K}} \equiv \frac{M_\bullet}{M_{\text{CND}}} \frac{R_{\text{CND}}^3}{a\sqrt{GM_\bullet a}} \quad (8)$$

to a very high eccentricity state. Unavoidable stellar scattering processes would in a short time destabilize an initially coherent stream of objects near the centre.

### 2.1.3 Combined perturbation

We now consider combined effect of the stellar cusp and the CND potentials on the long-term orbital evolution of the stellar orbit. The total, orbit-averaged potential

$$\overline{\mathcal{R}} = \overline{\mathcal{R}}_c + \overline{\mathcal{R}}_{\text{CND}} \quad (9)$$

still obeys axial symmetry, being independent on the nodal longitude. The picture, however, may be modified with respect to the case of solely ring-like perturbation. Considering the cusp of the late-type stars whose potential is approximated with (4), we find that the two types of topologies of the  $\overline{\mathcal{R}} = C$  isolines persist (see Fig. 1) but the onset of the circular-orbit instability depends now on two parameters, namely  $c$  and  $\mu \equiv M_c/M_{\text{CND}}$ . A nonzero mass of the stellar cusp stabilizes small eccentricity evolution and the critical

angle is pushed to larger values. For large enough  $\mu$ , the stability of the circular orbit is guaranteed for arbitrary value of  $c$  and hence orbits of an arbitrary inclination with respect to the CND symmetry plane. This is because the effects of the stellar cusp potential make the argument of pericentre circulate fast enough (significantly faster than the Kozai timescale), preventing thus secular increase of the eccentricity. An initially near-circular orbit maintains a very small value of  $e$  showing only small-amplitude oscillations. Fig. 2 shows critical inclination values, for which the circular orbit becomes necessarily unstable as a function of  $\mu$  and  $a/R_{\text{CND}}$  parameters (note the later factorizes out from the analysis when  $\mu = 0$ ). Importantly, there is a correlation between  $\mu$  and  $a/R_{\text{CND}}$  below which circular orbits of an arbitrary inclination are stable; for instance, data in Fig. 2 indicate that for  $\mu = 0.1$  any circular orbit with  $a \lesssim 0.12 R_{\text{CND}}$  is stable.

In conclusion, we observe that having enough mass in the late-type stellar cusp may produce strong enough perturbation to maintain small eccentricity of an initially near-circular orbit. With that said, we find it reasonable to make an important simplification within our analytic approach to the system of two (multiple) stars. Namely, we will further consider the stellar orbits to be circular during the whole evolution of the system. This prevents (together with the assumption of well separated orbits with constant semi-major axes) close encounters of the stars. In this case only, and under the assumption that there are no orbital resonances among the individual stars, the mutual interaction of the stars may be reasonably considered as a perturbation to the dominating potential of the SMBH. As we demonstrate in the next sections, this simple treatment provides useful insights into the evolution of the young-stream orbits even if they are generally non-circular.

## 2.2 Orbital evolution of circular orbits

Having discussed our assumptions about semi-major axes, eccentricity and pericentre of the stellar orbits, we may now turn to description of the evolution of the two remaining orbital elements – inclination and nodal longitude. We start with a model of two interacting stars and later generalize it to the case of an arbitrary number of stars. The major leap-forward in the model is that we now take into account also mutual gravitational effects of the two stars. On the contrary, note that the orbit-averaged potential energy (4) of the late-type stellar cusp depends on the semi-major axis and eccentricity only, and thus does not influence evolution of inclination and node. For that reason it drops from our analysis in this section.

The interaction potential energy  $\mathcal{R}_i(\mathbf{r}, \mathbf{r}')$  for two point sources of masses  $m$  and  $m'$  at relative positions  $\mathbf{r}$  and  $\mathbf{r}'$  with respect to the centre reads<sup>1</sup>

$$\mathcal{R}_i(\mathbf{r}, \mathbf{r}') = -\frac{Gmm'}{r} \sum_{\ell \geq 2} \alpha^\ell P_\ell(\cos S), \quad (10)$$

<sup>1</sup> Note that equation (10) provides the interaction energy as it appears in the equation of relative motion of stars with respect to the centre. Henceforth, the perturbation series start with a quadrupole term ( $\ell = 2$ ).

where  $P_\ell(x)$  are Legendre polynomials,  $\cos S \equiv \mathbf{r} \cdot \mathbf{r}' / rr'$  and  $\alpha \equiv r'/r$ . The series in the right-hand side of equation (10) converge for  $r' < r$ . Since we are going to apply (10) to the simplified case of two circular orbits, we may replace distances  $r$  and  $r'$  with the corresponding values of semi-major axis  $a$  and  $a'$ , such that  $\alpha = a'/a$  now (note that the orbit whose parameters are denoted with a prime is thus assumed interior). The averaging of the interaction energy over the uniform orbital motion of the stars about the centre, implying periodic variation of  $S$ , is readily performed by using the addition theorem for spherical harmonics. This allows us to decouple unit direction vectors in the argument of the Legendre polynomial  $P_\ell$  and easily obtain the required average of  $\mathcal{R}_i$  over the orbital periods of the two stars. After a simple algebra we obtain

$$\overline{\mathcal{R}_i} = -\frac{Gmm'}{a} \Psi(\alpha, \mathbf{n} \cdot \mathbf{n}'), \quad (11)$$

where  $\mathbf{n} = [\sin I \sin \Omega, -\sin I \cos \Omega, \cos I]^T$  and  $\mathbf{n}' = [\sin I' \sin \Omega', -\sin I' \cos \Omega', \cos I']^T$  are unit vectors normal to the mean orbital planes of the two stars, and

$$\Psi(\zeta, x) = \sum_{\ell \geq 2} [P_\ell(0)]^2 \zeta^\ell P_\ell(x). \quad (12)$$

As expected, the potential energy is only a function of: (i) the orbital semi-major axes through dependence on  $a$  and  $\alpha$ , and (ii) the relative configuration of the two orbits in space given by the scalar product  $\mathbf{n} \cdot \mathbf{n}'$ . Note also that the series in (12) contain only even multipoles  $\ell$  ( $P_\ell(0) = 0$  for  $\ell$  odd) and that they converge when  $\zeta < 1$ . However, a special care is needed when  $\zeta$  is very close to unity, thus the two stellar orbits are close to each other, when hundreds to thousands terms are needed to achieve sufficient accuracy. Still, we found it is very easy to set up an efficient computer algorithm, using recurrent relations between the Legendre polynomials, which is able to evaluate (12) and its derivatives. In practice, we select a required accuracy and the code truncates the series by estimating the remained terms. In fact, since our approach neglects small eccentricity oscillations of the orbits we are anyway not allowed to set  $\zeta = \alpha = a'/a$  arbitrarily close to unity. Theoretically, we should require

$$\alpha < 1 - \left( \frac{m + m'}{3M_\bullet} \right)^{1/3}, \quad (13)$$

by not letting the stars approach closer than the Hill radius of their mutual interaction. In the numerical examples we present below, this sets an upper limit  $\alpha < 0.98$ .

The formulation given above immediately provides potential energy of the star-CND interaction. In this case the stellar orbits are always interior to the CND with symmetry axis suitably chosen as the unity vector  $\mathbf{e}_z$  in the direction of the  $z$ -axis of our reference system. Unlike in Section 2.1.2, we restrict now to the case of circular orbit of the star but at the low computer-time expense we may include all multipole terms till specified accuracy is achieved. As a result the orbit-averaged interaction energy with the exterior stellar orbit is given by

$$\overline{\mathcal{R}_{\text{CND}}} = -\frac{GmM_{\text{CND}}}{R_{\text{CND}}} \Psi(a/R_{\text{CND}}, \cos I), \quad (14)$$

and similarly for the interior stellar orbit:

$$\overline{\mathcal{R}}'_{\text{CND}} = -\frac{Gm'M_{\text{CND}}}{R_{\text{CND}}} \Psi(a'/R_{\text{CND}}, \cos I'). \quad (15)$$

The total orbit-averaged potential energy perturbing motion of the two stars is then given by superposition of the three terms:

$$\overline{\mathcal{R}} = \overline{\mathcal{R}}_1 + \overline{\mathcal{R}}_{\text{CND}} + \overline{\mathcal{R}}'_{\text{CND}}. \quad (16)$$

Recalling that semi-major axis values are constant, eccentricity set to zero and thus argument of pericentre undefined, we are left to study dynamics of inclination  $I$  and  $I'$  and longitude of node  $\Omega$  and  $\Omega'$  values. Lagrange equations provide (see, e.g., Bertotti et al. 2003)

$$\frac{d \cos I}{dt} = -\frac{1}{mna^2} \frac{\partial \overline{\mathcal{R}}}{\partial \Omega}, \quad \frac{d\Omega}{dt} = \frac{1}{mna^2} \frac{\partial \overline{\mathcal{R}}}{\partial \cos I}, \quad (17)$$

$$\frac{d \cos I'}{dt} = -\frac{1}{m'n'a'^2} \frac{\partial \overline{\mathcal{R}}}{\partial \Omega'}, \quad \frac{d\Omega'}{dt} = \frac{1}{m'n'a'^2} \frac{\partial \overline{\mathcal{R}}}{\partial \cos I'}, \quad (18)$$

where  $n$  and  $n'$  denote mean motion frequencies of the two stars. Note the particularly simple, quasi-Hamiltonian form of equations (17) and (18). They can also be rewritten in a more compact way using the normal vectors  $\mathbf{n}$  and  $\mathbf{n}'$  to the respective orbit, namely

$$\frac{d\mathbf{n}}{dt} = \mathbf{n} \times \frac{\partial}{\partial \mathbf{n}} \left( \frac{\overline{\mathcal{R}}}{mna^2} \right), \quad (19)$$

$$\frac{d\mathbf{n}'}{dt} = \mathbf{n}' \times \frac{\partial}{\partial \mathbf{n}'} \left( \frac{\overline{\mathcal{R}}}{m'n'a'^2} \right). \quad (20)$$

Inserting here  $\overline{\mathcal{R}}$  from (16), we finally obtain

$$\frac{d\mathbf{n}}{dt} = \omega_{\text{I}} (\mathbf{n} \times \mathbf{n}') + \omega_{\text{CND}} (\mathbf{n} \times \mathbf{e}_z), \quad (21)$$

$$\frac{d\mathbf{n}'}{dt} = \omega'_{\text{I}} (\mathbf{n}' \times \mathbf{n}) + \omega'_{\text{CND}} (\mathbf{n}' \times \mathbf{e}_z), \quad (22)$$

where

$$\omega_{\text{I}} = -n \left( \frac{m'}{M_{\bullet}} \right) \Psi_x(\alpha, \mathbf{n} \cdot \mathbf{n}'), \quad (23)$$

$$\omega'_{\text{I}} = -n' \alpha \left( \frac{m}{M_{\bullet}} \right) \Psi_x(\alpha, \mathbf{n} \cdot \mathbf{n}'), \quad (24)$$

$$\omega_{\text{CND}} = -n \left( \frac{M_{\text{CND}}}{M_{\bullet}} \right) \Psi_x(a/R_{\text{CND}}, n_z), \quad (25)$$

$$\omega'_{\text{CND}} = -n' \left( \frac{M_{\text{CND}}}{M_{\bullet}} \right) \Psi_x(a'/R_{\text{CND}}, n'_z). \quad (26)$$

Note the frequencies in (23) to (26) depend on both  $\mathbf{n}$  and  $\mathbf{n}'$  through their presence in the argument of

$$\Psi_x(\zeta, x) \equiv \frac{d}{dx} \Psi(\zeta, x), \quad (27)$$

which breaks the apparent simplicity of the system of equations (21) and (22).

The coupled set of equations (21) and (22) acquires simple solutions in two limiting cases. First, when  $m = m' = 0$  (i.e. mutual interaction of stars is neglected) the two equations decouple and describe simple precession of  $\mathbf{n}$  and  $\mathbf{n}'$  about  $\mathbf{e}_z$  axis of the inertial frame with frequencies  $-\omega_{\text{CND}} \cos I$  and  $-\omega'_{\text{CND}} \cos I'$ . The sign minus of these frequencies recalls that the orbits precess in a retrograde sense when inclinations are less than  $90^\circ$  and vice versa. Both inclinations  $I$  and  $I'$  are constant. In the second limit, when

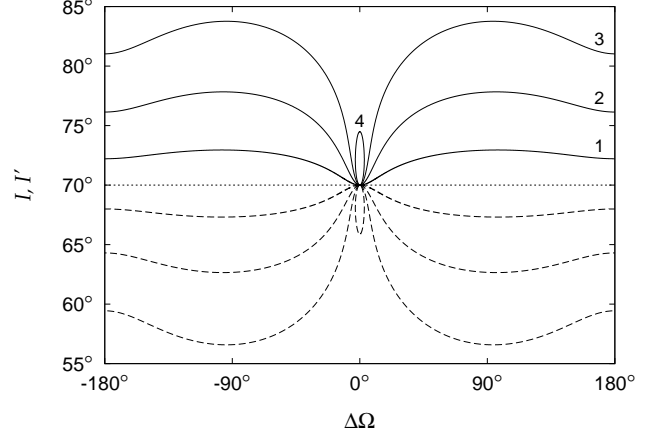


**Figure 3.** Isolines of the  $\overline{\mathcal{R}} = C_2$  integral in the  $I$  or  $I'$  vs.  $\Delta\Omega$  space. For sake of example we use orbits of two equal-mass stars ( $m' = m$ ) with semi-major axes  $a' = 0.04 R_{\text{CND}}$  and  $a = 0.05 R_{\text{CND}}$ . The mass of the CND is set to  $M_{\text{CND}} = 0.3 M_{\bullet}$ . The individual lines correspond to different values of stellar mass:  $m = 5 \times 10^{-7} M_{\bullet}$  (curves 1),  $m = 2 \times 10^{-6} M_{\bullet}$  (curves 2),  $m = 5 \times 10^{-6} M_{\bullet}$  (curves 3), and  $m = 9 \times 10^{-6} M_{\bullet}$  (curves 4). Both orbits have been given  $70^\circ$  inclination at  $\Delta\Omega = 0^\circ$  (i.e. initially coplanar and inclined orbits). Solid lines show inclination  $I'$  of the inner orbit, ‘the mirror-imaged’ dashed lines describe inclination  $I$  of the outer orbit.

$M_{\text{CND}} = 0$  (i.e. the circumnuclear torus is removed) the equations (21) and (22) obey a general integral of total angular momentum conservation

$$m\mathbf{n} + m'\alpha^{1/2}\mathbf{n}' = \mathbf{K}. \quad (28)$$

Both vectors  $\mathbf{n}$  and  $\mathbf{n}'$  then precess about  $\mathbf{K}$  with the same frequency

$$\omega_{\text{p}} = \frac{\omega_{\text{I}}}{m'\alpha^{1/2}} \frac{m + m'\alpha^{1/2}(\mathbf{n} \cdot \mathbf{n}')}{\sqrt{m^2 + m'^2\alpha + 2mm'\alpha^{1/2}(\mathbf{n} \cdot \mathbf{n}')}}, \quad (29)$$

keeping the same mutual configuration. In particular, initially coplanar orbits (i.e.  $\mathbf{n}$  and  $\mathbf{n}'$  parallel) would not evolve, which is in agreement with intuition.

Unfortunately, we were not able to find analytical solution to the (21) and (22) system except for these two situations described above. Obviously, it can be always solved using numerical methods as we shall discuss in Section 2.2.2.

### 2.2.1 Integrals of motion

In general, equations (21) and (22) have only two first integrals. Our assumptions about the circumnuclear torus mass distribution still provide a symmetry vector  $\mathbf{e}_z$ . Thus, while the total angular momentum  $\mathbf{K}$  is no more conserved now, its projection onto  $\mathbf{e}_z$  is still an integral of motion

$$m \cos I + m'\alpha^{1/2} \cos I' = C_1 = K_z. \quad (30)$$

Because  $m$ ,  $m'$  and  $\alpha$  are constant, equation (30) provides a direct constraint of how the two inclinations  $I$  and  $I'$  evolve. In particular, one can be expressed as a function of the other.

The quasi-Hamiltonian form of equations (17) and (18) readily results in a second integral of motion

$$\overline{\mathcal{R}}(\cos I, \cos I', \mathbf{n} \cdot \mathbf{n}') = C_2. \quad (31)$$

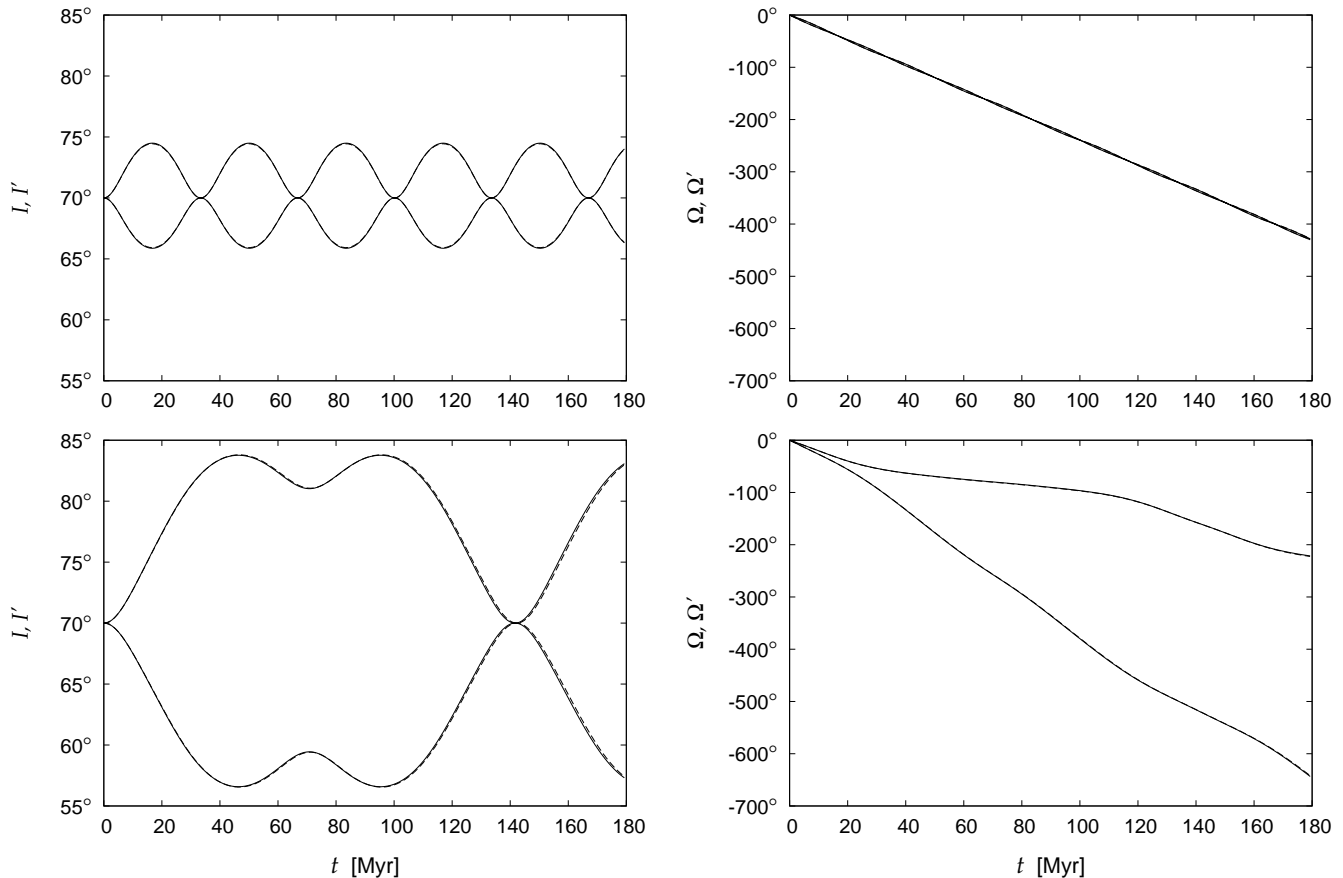


**Figure 4.** Evolution of the system of two stars in the compound potential of the central SMBH, spherical stellar cusp and axisymmetric CND. Solid lines represent solution of two-body equations (21) and (22), while the dashed lines show result of the direct numerical integration of the equations of motion. In each panel, upper and lower lines correspond to the inner and outer star, respectively. Common parameters for both examples are the same as in Fig. 3; in the upper panels, we set  $m = m' = 9 \times 10^{-6} M_{\bullet}$ , while in the lower ones  $m = m' = 5 \times 10^{-6} M_{\bullet}$ .

The list of arguments in  $\overline{\mathcal{R}}$ , as explicitly provided above, reminds that it actually depends on: (i) the inclination values  $I$  and  $I'$ , and (ii) the difference  $\Delta\Omega = \Omega - \Omega'$  of the nodal longitudes of the two interacting orbits. Using (30), the conservation of  $\overline{\mathcal{R}}$  thus provides a constraint between the evolution of  $I$  and  $\Delta\Omega$  (say). While not giving a solution of the problem, the constraint due to combination of first integrals (30) and (31) can still provide useful insights.

Fig. 3 illustrates how the first integrals help understanding several features of the orbital evolution for two interacting stars at distances  $a' = 0.04 R_{\text{CND}}$  and  $a = 0.05 R_{\text{CND}}$ . For sake of simplicity we also assume their mass is equal, hence  $m' = m$ , and the CND has been given mass  $M_{\text{CND}} = 0.3 M_{\bullet}$ . Data in this figure show constrained evolution of orbital inclinations  $I'$  (solid lines) and  $I$  (dashed lines) as a function of nodal difference  $\Delta\Omega$ . The two orbits were assumed to be initially coplanar ( $\Delta\Omega = 0^\circ$ ) with an inclination of  $I' = I = 70^\circ$ . A set of curves correspond to different values of stellar masses, from small (1) to larger values (4), which basically means increasing strength of their mutual gravitational interaction.

First, conservation of the  $e_z$ -projected orbital angular momentum, as given by equation (30), requires that increase in  $I'$  is compensated by decrease of  $I$ . This results in a near-

mirror-imaged evolution of the two inclinations. Using the first equation of (17), one finds

$$\frac{dI}{dt} = \frac{n}{\sin I} \frac{m'}{M_{\bullet}} \sin(\Omega - \Omega') \Psi_x(\alpha, \mathbf{n} \cdot \mathbf{n}'), \quad (32)$$

which straightforwardly implies that the outer stellar orbit is initially torqued to decrease its inclination while the inner orbit increases its inclination. This is because initially  $\mathbf{n} \cdot \mathbf{n}' \approx 1$ , and  $\Psi_x(\alpha, 1)$  is positive, and at the same time, precession of the nodes is dominated by interaction with the CND which makes the outward orbit node to drift faster (and hence  $\Omega - \Omega'$  is negative).

Second, Fig. 3 indicates there is important change in topology of the isolines  $\overline{\mathcal{R}} = C_2$  as the stellar masses overpass some critical value (about  $8.5 \times 10^{-6} M_{\bullet}$  in our example). For low-mass stars their mutual gravitational interaction is weak letting the effects of the CND dominate (curve 1). The orbits regularly precess with different frequency, given their different distance from the centre, and thus  $\Delta\Omega$  acquires all values between  $-180^\circ$  and  $180^\circ$ . The mutual stellar interaction produces only small inclination oscillation. As the stellar masses increase (curves 2 and 3) the inclination perturbation becomes larger. For super-critical values of  $m$  (curve 4) the isolines of constant  $\overline{\mathcal{R}}$  become only small loops about the origin. This means that  $\Delta\Omega$  is

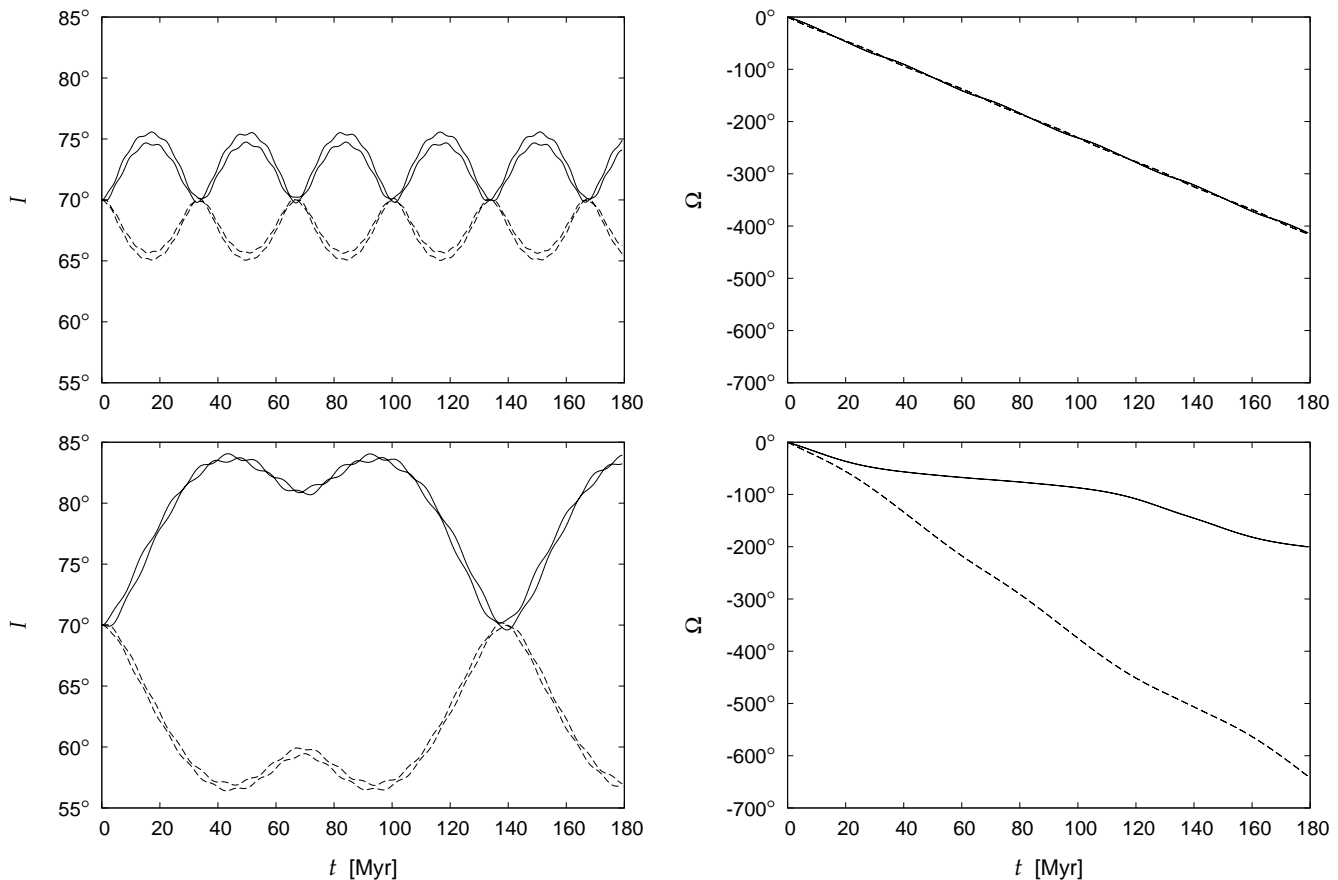


**Figure 5.** Evolution of the system of four stars in the compound potential of the central SMBH, spherical stellar cusp and axisymmetric CND. The stellar orbits form two couples. In both of them, the orbits have similar semi-major axes in order to mimic the system shown in Fig. 4. In each panel, upper and lower lines correspond to the inner and outer couple, respectively. The individual semi-major axes are for both examples set to  $a_1 = 0.0373 R_{\text{CND}}$ ,  $a_2 = 0.0408 R_{\text{CND}}$ ,  $a_3 = 0.0478 R_{\text{CND}}$ ,  $a_4 = 0.0511 R_{\text{CND}}$ . The other common parameters for both examples are the same as in Fig. 3; in the upper panels, we set  $m_1 = m_2 = m_3 = m_4 = 4.5 \times 10^{-6} M_{\bullet}$ , while in the lower ones  $m_1 = m_2 = m_3 = m_4 = 2.5 \times 10^{-6} M_{\bullet}$ .

bound to oscillate in a small interval near origin and inclination perturbation becomes strongly damped. Put in words, the gravitational coupling between the stars became strong enough to tightly couple the two orbits together. Note that they still collectively precess in space due to the influence of the CND.

### 2.2.2 Numerical solutions

In order to solve equations (21) and (22) numerically, we adopt a simple adaptive step-size 4.5th-order Runge-Kutta algorithm. Let us mention that our implementation of this algorithm conserves the value of both integrals of motion  $C_1$  and  $C_2$  with relative accuracy better than  $10^{-6}$ .

Two sample solutions are shown in Fig. 4. The upper panels represent evolution of two orbits with coupled precession which corresponds to the curve 4 in Fig. 3, while in the bottom panels we consider the case of lower-mass stars, whose orbits precess independently. This later mode corresponds to the curve 3 in Fig. 3. Beside the solution of the equations for mean orbital elements, we also show results of a full-fledged numerical integration of the particular configuration in the space of classical positions and momenta

$(\mathbf{r}, \mathbf{r}'; \mathbf{p}, \mathbf{p}')$ . Both solutions are nearly identical, which confirms validity of the secular perturbation theory used in this paper.

For sake of further discussion we find it useful to comment in a little more detail on the case of two, nearly independently precessing orbits (bottom panels on Fig. 4). In this case, the precession frequencies of the outer and inner star orbits are given by  $\omega_{\text{CND}}$  and  $\omega'_{\text{CND}}$  in equations (25) and (26). When truncated to the quadrupole ( $\ell = 2$ ) level, sufficient for the small value of  $a/R_{\text{CND}}$ , one has for the outer star orbit

$$\frac{d\Omega}{dt} \simeq -\frac{3 \cos I}{4 T_{\text{K}}}, \quad (33)$$

where  $T_{\text{K}}$  is given by (8). A similar formula holds for the inner star orbit denoted with primed variables. As seen in Fig. 3, and understood from the analysis of integrals of motion in Section 2.2.1, period of the evolution of the system of the two orbits is given implicitly by the difference of their precession rate:  $\Omega(T_{\text{char}}) - \Omega'(T_{\text{char}}) = 2\pi$ . The secular rate of nodal precession in (33) is not constant because the mutual gravitational interaction of the stars makes their orbital inclinations oscillate. However, in the zero approximation we may replace them with their initial values,  $I = I' = I_0$  which

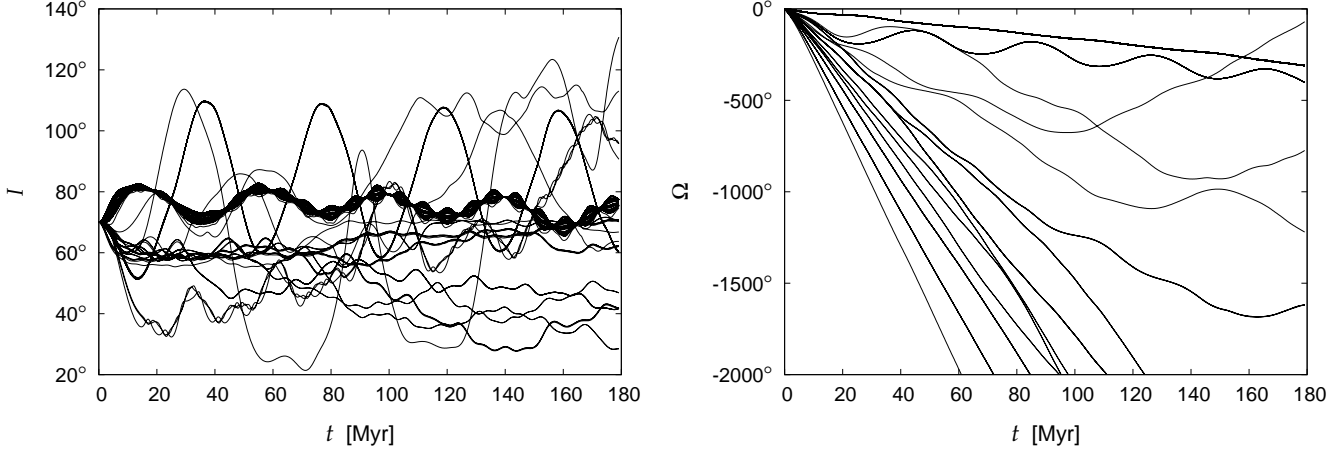


**Figure 6.** Evolution of the initially thin stellar disc of 100 stars in the compound potential of the central SMBH, spherical stellar cusp and axisymmetric CND. The values of orbital semi-major axes  $a_k$  in the disc range from  $0.02 R_{\text{CND}}$  to  $0.2 R_{\text{CND}}$  and their distribution obeys  $dN \propto a^{-1} da$ . The stellar masses are all equal with  $m = 5 \times 10^{-6} M_{\bullet}$  while the mass of the CND is set to  $M_{\text{CND}} = 0.3 M_{\bullet}$ . Initial inclination  $I_0$  of all the orbits with respect to the CND equals  $70^\circ$ .

gives an order of magnitude estimate

$$T_{\text{char}} \simeq \frac{8\pi}{3 \cos I_0} \left[ \frac{1}{T_K} - \frac{1}{T'_K} \right]^{-1}. \quad (34)$$

For the solution shown in the lower panels of Fig. 4, formula (34) gives  $T_{\text{char}} \approx 460$  Myr, in a reasonable agreement with the observed period of  $\approx 140$  Myr. When the orbital evolution is known (being integrated numerically), more accurate estimate can be obtained considering mean values of the inclinations

$$T_{\text{char}} \simeq \frac{8\pi}{3} \left[ \frac{\cos \bar{I}}{T_K} - \frac{\cos \bar{I}'}{T'_K} \right]^{-1}. \quad (35)$$

For the case of the solution of the lower panel of Fig. 4, with  $\bar{I} \approx 60^\circ$  and  $\bar{I}' \approx 80^\circ$ , formula (35) gives  $T_{\text{char}} \approx 120$  Myr.

### 2.2.3 Generalization for $N$ interacting stars

The previous formulation straightforwardly generalizes to the case of  $N$  stars orbiting the centre on circular orbits with semi-major axes  $a_k$  ( $k = 1, \dots, N$ ). This is because the potential energies of all pairwise interactions built the total

$$\bar{\mathcal{R}}_i = -\frac{1}{2} \sum_{k \neq l} \frac{Gm_k m_l}{a_{kl}} \Psi(\alpha_{kl}, \mathbf{n}_k \cdot \mathbf{n}_l), \quad (36)$$

where  $m_k$  is the mass of the  $k$ -th star,  $a_{kl} = \min(a_k, a_l)$ ,  $\alpha_{kl} = \min(a_k, a_l)/\max(a_k, a_l)$  and  $\mathbf{n}_k$  is the normal vector to the orbital plane of the  $k$ -th star. Similarly, interaction with the CND is simply given by

$$\bar{\mathcal{R}}_{\text{CND}} = -\sum_k \frac{Gm_k M_{\text{CND}}}{a_k} \Psi(a_k/R_{\text{CND}}, \mathbf{n}_k \cdot \mathbf{e}_z). \quad (37)$$

The total potential energy of perturbing interactions is

$$\bar{\mathcal{R}} = \bar{\mathcal{R}}_i + \bar{\mathcal{R}}_{\text{CND}}, \quad (38)$$

and the equations of orbital evolution now read

$$\frac{d\mathbf{n}_k}{dt} = \mathbf{n}_k \times \frac{\partial}{\partial \mathbf{n}_k} \left( \frac{\bar{\mathcal{R}}}{m_k n_k a_k^2} \right), \quad (39)$$

for  $k = 1, \dots, N$  ( $n_k$  is the frequency of the unperturbed mean motion of the  $k$ -th star about the centre). Their first integrals then can be written as

$$\sum_k m_k n_k a_k^2 (\mathbf{n}_k \cdot \mathbf{e}_z) = C_1 = K_z \quad (40)$$

and

$$\bar{\mathcal{R}} = C_2. \quad (41)$$

Due to mutual interaction of multiple stars, solutions of equations (39) represent, in general, an intricate orbital evolution, whose course is hardly predictable as it strongly depends upon the initial setup. Our numerical experiments show, however, that it is still possible to identify several qualitative features which remain widely valid. For instance, a group of orbits with small separations may orbitally couple together and effectively act as a single orbit in interaction with the rest of the stellar system.

This is demonstrated in Fig. 5 which shows two sample solutions of equations (39) for a system of two such groups. For sake of clarity, each group consists only of two orbits. Individual semi-major axes are, for both solutions, set to  $a_1 = 0.0373 R_{\text{CND}}$ ,  $a_2 = 0.0408 R_{\text{CND}}$ ,  $a_3 = 0.0478 R_{\text{CND}}$ ,  $a_4 = 0.0511 R_{\text{CND}}$  in order to mimic the two-orbits models from Fig. 4. For the same reason, all the individual masses are considered equal,  $m_1 = m_2 = m_3 = m_4$ , and set to  $2.5 \times 10^{-6} M_{\bullet}$  in the lower panels, while for the upper panels we assume  $4.5 \times 10^{-6} M_{\bullet}$ . The other parameters remain identical to the case of the two-orbits models. As we can see (cf. Figs 5 and 4), the dynamical impact of each coupled pair of orbits upon the rest of the stellar system is equivalent to the effect of the corresponding single orbit if both the total mass and semi-major axis of the pair are appropriate. The individual orbits within each pair then naturally oscillate about the single-orbit solution according to their mutual interaction. This conclusion remains valid even in more complicated systems as we shall show in the next section.

### 3 APPLICATION TO THE YOUNG STELLAR SYSTEM IN THE SGR A\* REGION

In order to illustrate the complexity of solutions of equations (39), let us now analyze the evolution of a system which contains an initially thin stellar disc with a distribution of semi-major axes of the orbits  $dN \propto a^{-1}da$ . As we can see in Fig. 6, the oscillations of the orbital inclinations no longer have the simple patterns which we observed for the models discussed in the previous paragraphs. On the other hand, we still can identify a well defined group of orbits which coherently change their orientation with respect to the CND. These orbits thus form a rather thin disc during the whole monitored period of time. It turns out that they represent the innermost parts of the initial disc where the separations of the neighbouring orbits are small enough for their mutual interaction to couple them together.

The configuration considered in Fig. 6 roughly matches the main qualitative features of an astrophysical system which is observed in the centre of the Milky Way. It contains a group of early-type stars orbiting the SMBH on nearly Keplerian orbits. Observations suggest that about one half of them form a coherently rotating disc-like structure with estimated surface density profile  $\Sigma \propto R^{-2}$  (Paumard et al. 2006; Lu et al. 2009; Bartko et al. 2009) which implies the above considered distribution of semi-major axes. The rest of the early-type stars then appear to be on randomly oriented orbits. Both the origin and observed configuration of these stars represent rather puzzling questions. Due to strong tidal field of the SMBH, it is impossible for a star to be formed in this region by any standard star formation mechanism. On the other hand, as the observed stars are assumed to be young, no usual transport mechanism is efficient enough to bring them from farther regions, where their formation would be less intricate, within their estimated lifetime. One of the most promising scenarios of their origin thus considers formation in situ, via fragmentation of a self-gravitating gaseous disc (Levin & Beloborodov 2003). However, since this process naturally forms stars in a single disc-like structure, it does not explain the origin of the stars observed outside the disc. Hence, in order to justify the in-disc scenario of the formation of the early-type stars in the Galactic Centre, some mechanism that may have dragged some of them out from the parent stellar disc plane is needed.

In our previous paper (Haas et al. 2011), we have discussed a possibility that all the early-type stars had been born in a single disc which has been, subsequently, partially disrupted by the gravity of the CND. We have considered the same configuration of the sources of the gravitational field as in the current paper and followed the evolution of the disc by means of direct  $N$ -body integration. We have observed coherent evolution of the inner dense part of the disc which exhibited a tendency to increase its inclination with respect to the CND. On the other hand, most of the orbits of the outer parts of the initially coherently rotating disc precessed independently due to the influence of the CND and, consequently, became detached from the parent structure. This behaviour is in accord with the analysis presented in the current paper.

Furthermore, we can now calculate the order of magnitude characteristic time-scale for the ‘canonical’ model of Haas et al. (2011) whose system parameters read:  $M_{\bullet} =$

$4 \times 10^6 M_{\odot}$ ,  $R_{\text{CND}} = 1.8 \text{ pc}$ ,  $M_{\text{CND}} = 0.3 M_{\bullet}$ ,  $M_c = 0.03 M_{\bullet}$ , and  $I_0 = 70^{\circ}$ . In order to determine the rough time estimate, we use formula (34). As this formula has been derived for a system of two stars, we replace the stellar disc with two characteristic particles at certain radii  $a'$ ,  $a$  in the sense of Section 2.2.3. For this purpose, let us divide the stars in the disc into two groups according to their initial distance from the centre and define  $a'$  and  $a$  as the radii of the orbits of the median stars in the inner and outer group, i.e.  $a' = 0.06 \text{ pc}$  and  $a = 0.23 \text{ pc}$ . Inserting these values into formula (34), we obtain  $T_{\text{char}} \approx 37 \text{ Myr}$  for the ‘canonical’ model. This value is in order of magnitude agreement with the estimated age of the early-type stars,  $\approx 6 \text{ Myr}$  (Paumard et al. 2006), since the core of the disc reaches its maximal inclination with respect to the CND already after a fraction of period  $T_{\text{char}}$  as can be seen in Figs. 5 and 6.

Let us emphasize that the results reported in our previous paper (Haas et al. 2011) have been acquired by means of full-fledged numerical integration of equations of motion. As a consequence, both the eccentricities and semi-major axes of the individual stellar orbits in the disc have been naturally undergoing a significant evolution due to two-body relaxation of the disc. Moreover, our prior numerical computations have also confirmed that results similar to those obtained for the ‘canonical’ model are valid for a wide set of models with different system parameters, including the case with zero mass,  $M_c$ , of the spherical cusp of the late-type stars. In the later case, the orbital eccentricities and inclinations within the stellar disc are subject to high-amplitude Kozai oscillations. In conclusion, it appears that the inner part of the disc may evolve coherently for a certain period of time even when we cannot assume neither zero nor small eccentricity of the stellar orbits. We, therefore, suggest that also some of the key qualitative predictions of the semi-analytic theory developed in the current paper under the simplifying assumption of circular orbits may be carefully applied to more general, non-circular systems.

Finally, let us mention that, in addition to the core of the disc, less significant groups of orbits with coherent secular evolution may exist even in the outer parts of the disc if their separations are small enough. Our semi-analytic approach thus admits possible existence of secondary disc-like structures in the observed young stellar system which has indeed been discussed by several authors (Genzel et al. 2003; Paumard et al. 2006; Bartko et al. 2009).

### 4 CONCLUSIONS

We have investigated the secular orbital evolution of a system of  $N$  mutually interacting stars on nearly-circular orbits around the dominating central mass, considering the perturbative gravitational influence of a distant axisymmetric source and an extended spherical potential. Given the spherical potential is strong enough, we have shown that the secular evolution of initially circular orbits reduces to the evolution of inclinations and nodal longitudes. The spherical potential itself can then be factorized out from the outgoing momentum equations. Since we have not been able, in a general case, to solve the derived equations analytically, we have set up an integrator for their efficient numerical solution. The acquired results have then been, in order to

confirm their validity, compared with the corresponding full-fledged numerical integrations in the space of classical positions and momenta, showing a remarkable agreement.

Some fundamental features of the possible solutions of the new equations can be understood by an analysis of the integrals of motion. In the case of the simplest possible system of two stars interacting in the considered perturbed potential, we have identified two qualitatively different modes of its secular evolution. If the interaction of the stars is weak (yet still non-zero), the secular evolution of their orbits is dominated by an independent nodal precession. Difference of the individual precession rates then determines the period of oscillations of the orbital inclinations. On the other hand, when the gravitational interaction of the stars is sufficiently strong (depending on their mass and the radii of their orbits), the secular evolution of the orbits becomes dynamically coupled and, consequently, they precess coherently around the symmetry axis of the gravitational potential. Oscillations of the orbital inclinations are, in this case, considerably damped.

We have further confirmed, by means of numerical integration of the derived momentum equations, that the coupling of strongly interacting orbits is a generic process that may occur even in more complex  $N$ -body systems. In particular, a subset of stars with strong mutual interaction evolves coherently and, as a result, its dynamical impact upon the rest of the  $N$ -body system is similar to the effect of a single particle of suitable mass and orbital radius.

As an example, we have investigated evolution of a disc-like structure that roughly models the young stellar system which is observed in the Galactic Centre. It has turned out that the semi-analytic work presented in this paper provides a physical background for understanding of the processes discovered, by means of full  $N$ -body integration, in Haas et al. (2011). Namely, coupling of the strongly interacting stars from the inner parts of the disc leads to their coherent orbital evolution, which allows us to observe a disc-like structure even after several million years of dynamical evolution in the tidal field of the CND. Orientation of this surviving disc then inevitably changes towards higher inclination with respect to the CND, which is in accord with the observations. On the other hand, stellar orbits from the outer parts of the disc evolve individually, being gradually stripped out from the parent thin disc structure. Hence, it appears possible for the puzzle of the origin of the young stars in the Galactic Centre to be solved by the hypothesis of their formation via fragmentation of a single gaseous disc, as already suggested in Šubr, Schovancová & Kroupa (2009) and Haas et al. (2011).

Note that, beside the physical explanation of the processes observed in our previous work, the current approach would be, due to its low numerical demands, useful for extensive scanning of the parameter space in order to confront our model with the observations more thoroughly. This is going to be a subject of our future work when more accurate observational data will be available.

Finally, let us mention that our semi-analytic model has been developed under several simplifying assumptions. Most importantly, the torus CND has been considered stationary and the cusp of the late-type stars spherically symmetric. If any of these assumptions were violated, the results might be more or less affected. For example, a possible anisotropy

of the cusp of the late-type stars due to chance alignment of some of its stars would break its spherical symmetry. In that case, the resulting gravitational torques might have a considerable impact on the dynamical evolution of the stellar disc as shown by Kocsis & Tremaine (2011). However, since the current observational data do not show evidence for such violations, we may consider our model physically plausible. Moreover, the currently available data do suggest roughly perpendicular mutual orientation of the CND and the stellar disc, which is in accord with the predictions of both our numerical and semi-analytic model. We consider this as a supporting argument for our findings.

## ACKNOWLEDGMENTS

We thank the anonymous referee for useful comments. This work was supported by the Czech Science Foundation via grants GACR-205/09/H033, GACR-205/07/0052 and GACR-202/09/0772, from the Research Program MSM0021620860 of the Czech Ministry of Education, and also from project 367611 of the Grant Agency of Charles University in Prague. The calculations were performed on the computational cluster Tiger at the Astronomical Institute of Charles University in Prague (<http://sirrah.troja.mff.cuni.cz/tiger>).

## REFERENCES

- Bahcall J. N., Wolf R. A., 1976, *ApJ*, 209, 214
- Bartko H. et al., 2009, *ApJ*, 697, 1741
- Bartko H. et al., 2010, *ApJ*, 708, 834
- Bertotti B., Farinella P., Vokrouhlický D., 2003, *Physics of the Solar System*, Kluwer Academic Publishers, Dordrecht, The Netherlands
- Christopher M. H., Scoville N. Z., Stolovy S. R., Yun M. S., 2005, *ApJ*, 622, 346
- Do T., Ghez A. M., Morris M. R., Lu J. R., Matthews K., Yelda S., Larkin J., 2009, *ApJ*, 703, 1323
- Eisenhauer F. et al., 2005, *ApJ*, 628, 246
- Genzel R. et al., 2003, *ApJ*, 594, 812
- Ghez A. M. et al., 2003, *ApJ*, 586, L127
- Ghez A. M., Salim S., Hornstein S. D., Tanner A., Lu J. R., Morris M., Becklin E. E., Duchêne G., 2005, *ApJ*, 620, 744
- Gillessen S., Eisenhauer F., Trippe S., Alexander T., Genzel R., Martins F., Ott T., 2009a, *ApJ*, 692, 1075
- Gillessen S., Eisenhauer F., Fritz T. K., Bartko H., Dodds-Eden K., Pfuhl O., Ott T., Genzel R., 2009b, *ApJ*, 707, L114
- Haas J., Šubr L., Kroupa P., 2011, *MNRAS*, 412, 1905
- Ivanov P. B., Polnarev A. G., Saha P., 2005, *MNRAS*, 358, 1361
- Karas V., Šubr L., 2007, *A&A*, 470, 11
- Kocsis B., Tremaine S., 2011, *MNRAS*, 412, 187
- Kozai Y., 1962, *AJ*, 67, 591
- Levin Y., Beloborodov A. M., 2003, *ApJ*, 590, L33
- Lidov M. L., 1962, *Planetary and Space Sci.*, 9, 719
- Lu J. R., Ghez A. M., Hornstein S. D., Morris M. R., Becklin E. E., Matthews K., 2009, *ApJ*, 690, 1463

- Morbidelli A., 2002, *Modern Celestial Mechanics*, Taylor & Francis, London and New York
- Paumard T. et al., 2006, *ApJ*, 643, 1011
- Schödel R. et al., 2007, *A&A*, 469, 125
- Šubr L., Schovancová J., Kroupa P., 2009, *A&A*, 496, 695
- Yelda S., Ghez A. M., Lu J. R., Do T., Clarkson W., Matthews K., 2010, in M. Morris, D. Q. Wang, F. Yuan, eds, *Proc. Conf., The Galactic Center: A Window on the Nuclear Environment of Disk Galaxies*. Astron. Soc. Pac., San Francisco
- Yokoyama T., Santos M. T., Cardin G., Winter O. C., 2003, *A&A*, 401, 763

This paper has been typeset from a  $\text{\TeX}$ / $\text{\LaTeX}$  file prepared by the author.